

# Preoperative [<sup>11</sup>C]methionine PET to personalize treatment decisions in patients with lower-grade gliomas

Gaia Ninatti, Martina Sollini<sup>✉</sup>, Beatrice Bono, Noemi Gozzi, Daniil Fedorov, Lidija Antunovic, Fabrizia Gelardi, Pierina Navarria, Letterio S. Politi, Federico Pessina<sup>†,✉</sup>, and Arturo Chiti<sup>†</sup>

*Department of Biomedical Sciences, Humanitas University, Pieve Emanuele, Milan, Italy (G.N., M.S., B.B., D.F., F.G., L.S.P., F.P., A.C.); Diagnostic Imaging Department, IRCCS Humanitas Research Hospital, Rozzano, Milan, Italy (M.S., N.G., L.A., F.G., L.S.P., A.C.); Neurosurgery Department, IRCCS Humanitas Research Hospital, Rozzano, Milan, Italy (B.B., F.P.); Radiotherapy and Radiosurgery Department, IRCCS Humanitas Research Hospital, Rozzano, Milan, Italy (P.N.)*

<sup>†</sup>These authors share the last authorship for this work.

**Corresponding Author:** Martina Sollini, PhD, Department of Biomedical Sciences, Humanitas University, Via Rita Levi Montalcini 4, 20090 Pieve Emanuele—Milan, Italy ([martina.sollini@hunimed.eu](mailto:martina.sollini@hunimed.eu)).

## Abstract

**Background.** PET with radiolabeled amino acids is used in the preoperative evaluation of patients with glial neoplasms. This study aimed to assess the role of [<sup>11</sup>C]methionine (MET) PET in assessing molecular features, tumor extent, and prognosis in newly diagnosed lower-grade gliomas (LGGs) surgically treated.

**Methods.** One hundred and fifty-three patients with a new diagnosis of grade 2/3 glioma who underwent surgery at our Institution and were imaged preoperatively using [<sup>11</sup>C]MET PET/CT were retrospectively included. [<sup>11</sup>C]MET PET images were qualitatively and semi-quantitatively analyzed using tumor-to-background ratio (TBR). Progression-free survival (PFS) rates were estimated using the Kaplan-Meier method and Cox proportional-hazards regression was used to test the association of clinicopathological and imaging data to PFS.

**Results.** Overall, 111 lesions (73%) were positive, while thirty-two (21%) and ten (6%) were isometabolic and hypometabolic at [<sup>11</sup>C]MET PET, respectively. [<sup>11</sup>C]MET uptake was more common in oligodendrogliomas than *IDH*-mutant astrocytomas (87% vs 50% of cases, respectively). Among [<sup>11</sup>C]MET-positive gliomas, grade 3 oligodendrogliomas had the highest median TBR<sub>max</sub> (3.22). In 25% of patients, PET helped to better delineate tumor margins compared to MRI only. In *IDH*-mutant astrocytomas, higher TBR<sub>max</sub> values at [<sup>11</sup>C]MET PET were independent predictors of shorter PFS.

**Conclusions.** This work highlights the role of preoperative [<sup>11</sup>C]MET PET in estimating the type of suspected LGGs, assessing tumor extent, and predicting biological behavior and prognosis of histologically confirmed LGGs. Our findings support the implementation of [<sup>11</sup>C]MET PET in routine clinical practice to better manage these neoplasms.

## Key Points

- Preoperative [<sup>11</sup>C]MET PET may provide crucial information for the characterization of suspected lower-grade glioma type.
- [<sup>11</sup>C]MET PET and MRI provide complementary information on tumor extent before surgery.
- [<sup>11</sup>C]MET PET has independent prognostic value in patients with *IDH*-mutant astrocytomas.

## Importance of the Study

[<sup>11</sup>C]methionine (MET) PET is widely used to complement to MRI in the preoperative management of patients with gliomas. However, there is still no clear evidence for its added value in lower-grade gliomas (LGGs). This study is the first comprehensive investigation on the diagnostic and prognostic value of amino acid PET in LGGs stratified according to WHO type and other known prognostic factors. We showed that [<sup>11</sup>C]MET PET provides important data for the prospective assessment of suspected LGG type and

grade before the availability of a histomolecular diagnosis. Additionally, we demonstrated the complementary role of MRI and [<sup>11</sup>C]MET PET in delineating of tumor margins before surgery. Finally, for the first time, our findings proved that [<sup>11</sup>C]MET PET has an independent prognostic role in LGG patients with *IDH*-mutant astrocytomas. Our results support the routine implementation of [<sup>11</sup>C]MET PET to personalize treatment decisions and optimize patient management in newly diagnosed LGGs.

World Health Organization (WHO) grade 2/3 gliomas, known as lower-grade gliomas (LGGs), are primary central nervous system (CNS) neoplasms that together account for about 15–20% of all malignant brain tumors.<sup>1</sup> LGGs constitute a group of very heterogeneous entities characterized by different pathological behavior and biological aggressiveness. As of 2007,<sup>2</sup> grade 2 and 3 diffuse gliomas were classified and graded based on histological appearance into tumors of astrocytic lineage, oligodendrocytic tumors, and mixed gliomas. With the advent of the molecular era, a better understanding of the genetic basis of gliomagenesis has led to new CNS WHO classifications<sup>3,4</sup> breaking with the traditional microscopy-based diagnosis and incorporating molecular parameters. Recognized key molecular diagnostic markers in LGGs include isocitrate dehydrogenase 1 and 2 (*IDH1/2*) genes mutation, 1p/19q codeletion, *ATRX* mutation, and *TP53* mutation. According to the 2021 CNS WHO classification<sup>4</sup> and cIMPACT-NOW recommendations,<sup>5</sup> these molecular biomarkers allow to classify LGGs into two types with solid prognostic value, namely *IDH*-mutant and 1p/19q-codeleted oligodendrogliomas, and *IDH*-mutant astrocytomas. The new integrated diagnosis has brought key achievements in prognostication for LGGs.<sup>6,7</sup> Indeed, apart from patient-specific prognostic factors (i.e. age, performance status, neurological deficits) and therapy-related prognostic factors (i.e. extent of tumor resection, postoperative treatments), molecular and genetic factors associated with more favorable outcomes have been identified.

Brain magnetic resonance imaging (MRI) is the modality of choice for diagnosing, preoperative workup, and surgical planning of a suspected LGG. However, in the latest years, amino acid positron emission tomography (PET) with [<sup>11</sup>C]methionine (MET) has been introduced as a complement to MRI in the clinical management of LGGs. [<sup>11</sup>C]MET PET is indeed able to provide complementary information on tumor extent/biology and intratumoral heterogeneity to that offered by MRI.<sup>8,9</sup> Accordingly, it may identify diseases with more aggressive behavior and growth pattern, and thus at higher risk of recurrence after treatment. However, to the best of our knowledge, the added value of preoperative [<sup>11</sup>C]MET PET has never been studied in a large series of lower-grade glioma patients. Moreover, although previous studies and recently published guidelines<sup>10–14</sup> support the use of amino acid PET at baseline to differentiate high- and low-grade lesions, to delineate tumor extent

before surgery or radiotherapy, to guide stereotactic biopsy, and for prognostication, several constraints (e.g. variability in methodologies, heterogeneity of populations) hampers its routinely use in the pre-surgical setting.<sup>15</sup> The present study aimed to evaluate the role of [<sup>11</sup>C]MET PET in assessing histopathological and molecular features, tumor extent, and prognosis in patients with newly diagnosed WHO grade 2/3 astrocytic and oligodendroglial tumors.

## Materials and Methods

### Study Design and Patient Population

This was a single-center, observational, retrospective study.

We included patients with a newly diagnosed, histologically-proven lower-grade glioma who underwent surgical resection at our Hospital between July 2011 and January 2021 and were imaged preoperatively using [<sup>11</sup>C]MET PET/CT and MRI.

The following exclusion criteria were used: (1) treatment (chemotherapy, radiotherapy, chemoradiotherapy) before PET imaging; (2) biopsy before PET imaging; (3) lower-grade glioma with no precise histological grading; (4) interval between PET imaging and surgical resection  $\geq 100$  days.

We collected demographic, clinical, histomolecular, imaging, treatment, and outcome data.

This study was approved by the IRCCS Humanitas Research Hospital Ethics Committee [approval n. 19/21, 23.03.2021] and was conducted under the Declaration of Helsinki. Due to the observational retrospective design of the study, patients' signature of a specific informed consent was waived.

### Magnetic Resonance Imaging

For all patients, volumetric MRI sequences were acquired before surgery using a 3 Tesla Siemens MAGNETOM Verio MRI scanner (Siemens Medical Systems). The preoperative MRI protocol included T1-weighted pre- and postgadolinium, T2-weighted, and FLAIR scans and, in most cases, DWI, fMRI, and DTI. Postoperative MRI at 48 hours and two months were obtained to estimate the extent of resection.

## [<sup>11</sup>C]MET PET Imaging

All patients were imaged preoperatively using [<sup>11</sup>C]MET PET <100 days before surgery. L-[<sup>11</sup>C-methyl]-methionine was synthesized on-site. Brain images were acquired 10 minutes after the intravenous injection of 300–500 MBq of the radiopharmaceutical. Three-dimensional PET/CT images were acquired according to the hospital protocol with either a GE Discovery 690 (GE Healthcare, Waukesha, Wisconsin, USA) or a Siemens Biograph 6 (Siemens Medical Systems, Erlangen, Germany) scanner.

## Image Analysis

[<sup>11</sup>C]MET PET images were qualitatively and semi-quantitatively analyzed.

At visual analysis, exams were considered positive in case of increased radiopharmaceutical uptake at the lesion level. Negative exams were further classified as isometabolic or hypometabolic, depending on whether the radiotracer uptake in the region of interest was equal or less than in the normal surrounding brain. Two authors (GN, MS) independently performed the visual image analysis. A third (LA) and fourth (FG) authors resolved any discordance in interpretation using the majority voting.

The semi-quantitative analysis was performed using the tumor-to-background ratio (TBR). In positive exams, we also computed the metabolic tumor volume (MTV).  $TBR_{max}$  and  $TBR_{mean}$  were calculated as ratios between  $SUV_{max}$  and  $SUV_{mean}$  of the tumor volume of interest, respectively, and uptake values of normal tissue, used as reference. We used a crescent-shaped volume of interest in the contralateral brain to assess background activity, which has been proposed as the most reliable method for background activity assessment in <sup>18</sup>F-FET PET imaging.<sup>16</sup> For all positive exams, a 3-dimensional auto-contouring process using the suggested<sup>9</sup>  $TBR_{max}$  threshold >1.3 was used to segment of the MTV with LIFEx software ([www.lifexsoft.org](http://www.lifexsoft.org)).<sup>17</sup>

All positive [<sup>11</sup>C]MET PET scans with segmented MET PET-based tumor volumes of interest were co-registered with the preoperative MRI using the iPlan Cranial software (Brainlab AG). Spatial comparison between (1) MET PET-based and T2-FLAIR-based tumor volumes and (2) MET PET-based tumor volumes and postcontrast T1-based tumor volumes—for contrast-enhancing gliomas—was performed. Two authors (G.N. and B.B.) visually assessed the spatial correlation between the MET PET-based tumor volumes and the T2-FLAIR-based and postcontrast T1-based tumor volumes following these criteria: (a) MET PET-based tumor volume inside T2-FLAIR-based tumor volume, (b) MET PET-based tumor volume outside T2-FLAIR-based tumor volume, (c) MET PET-based tumor volume inside postcontrast T1-based tumor volume, and (d) MET PET-based tumor volume outside postcontrast T1-based tumor volume.

## Surgery

All patients gave written informed consent for the neuro-surgical procedure.

In all cases, surgery aimed at maximal safe resection of the lesion. Microsurgical tumor removal was performed with the aid of neuronavigation with co-registered pre-operative MRI, CT, and PET series, and with the help of intraoperative neurophysiological monitoring and functional brain mapping.

The excised tumor volume was assessed comparing the preoperative volume of the lesion on FLAIR sequences with the postoperative (at 48 hours and two months after surgery) volume using iPlan Cranial software (Brainlab AG). According to the percentage of removed tumor volume, the extent of resection was classified as complete (≥95%, which include supra-total and gross total resection), and incomplete (30–94%, which include subtotal and partial resection).

## Histomolecular Analysis

Neuropathological evaluation of tumor specimens obtained by surgical resection and stained with hematoxylin and eosin was performed according to the 2007 and 2016 WHO Classification of Tumors of the Central Nervous System. Diagnoses were updated following the new 2021 CNS WHO indications, and patients re-classified accordingly.

*IDH1/2* and 1p/19q statuses were determined for all patients included in the study. In most cases, additional molecular analyses including the Ki-67 index, *ATRX* and *TP53* statuses, and *MGMT* promoter methylation status.

The presence of *IDH1/2* mutation was assessed by IHC using anti-*IDH1* R132H antibodies. In case of negative stain, for diagnoses performed after 2014, *IDH1* and *IDH2* sequencing was added as a diagnostic confirmation.

FISH was used for the identification of 1p/19q codeletion. 1p/19q codeletion was reported in presence of at least 20% (pre-specified cutoff) of tumor cells with a deleted signal.

The Ki-67 proliferation index was determined by IHC using anti-MIB-1 antibodies.

*ARTX* and *TP53* mutations were evaluated by IHC.

*MGMT* promoter methylation status was assessed by pyrosequencing.

Following the 2021 CNS WHO recommendations, tumor grading and molecular markers were used to classify LGGs into *IDH*-mutant and 1p/19q-codeleted WHO grade 2 and 3 oligodendrogliomas, and *IDH*-mutant and 1p/19q-non codeleted WHO grade 2 and 3 astrocytomas.

## Postoperative Treatments and Outcome Evaluation

A neuro-oncology multidisciplinary team evaluated the need of any postoperative treatment on a case-by-case basis, according to the disease histomolecular profile, the EOR, and to patient intrinsic factors, namely age and performance status.

Follow-up neurological examination and MRI were performed at 3–6 months intervals depending on the histomolecular diagnosis. Disease recurrence or progression after treatment was defined according to the Response Assessment in Neuro-Oncology (RANO) criteria.<sup>18,19</sup>

## Statistical Analysis

In the descriptive analysis, quantitative variables were tested for normal distribution by Shapiro-Wilk test. In case of normal distribution, mean and standard deviation were reported, while in case of non-normal distribution, median and interquartile range (IQR) were used. Kruskal-Wallis H test was used to compare the median of quantitative variables. Ordinal and categorical variables were compared by the chi-squared ( $\chi^2$ ) test. For multiple testing, Bonferroni correction was applied. *P*-values <.05 were considered statistically significant.

For the visual image analysis, interobserver agreement was estimated using Cohen's kappa ( $\kappa$ ), and rated as none (0–0.20), minimal (0.21–0.39), weak (0.40–0.59), moderate (0.60–0.79), strong (0.80–0.90), and almost perfect (>0.90).<sup>20</sup>

Progression-free survival (PFS) time was calculated from surgical intervention to disease progression/recurrence or death from any cause. Kaplan-Meier curves analyzed PFS rates. A log-rank test (Mantel-Cox) was run to compare survival curves. Cox proportional-hazards regression was used to test the association of demographic, clinical, histomolecular, and imaging data to PFS. Significant variables on univariate analysis and variables with a well-known prognostic value were selected for the multivariate Cox regression analysis. *P*-values <.05 were considered statistically significant. Stata MP (StataCorp LP, TX, USA) software, version 14.0 and GraphPad PRISM, version 9.0.0 were used.

## Results

### Patient Characteristics

Two hundred and one patients were selected using the above-mentioned criteria. However, 48 out of 201 gliomas were re-classified as glioblastoma according to the 2021 CNS WHO recommendations, and therefore excluded from the analysis. Collectively, 153 patients with a newly diagnosed, histologically confirmed LGG fulfilling selection criteria were included in the study. LGGs were classified in two types—oligodendrogliomas, *IDH*-mutant and 1p/19q-codeleted (61%), and astrocytomas, *IDH*-mutant (39%)—following the indications provided by the 2021 CNS WHO classification. Diagnoses made applying the 2007 and 2016 WHO CNS criteria (*n* = 153) were modified according to the new 2021 CNS WHO. Discrepancies were present in 26 cases: in particular, we re-classified 7 oligoastrocytomas as oligodendrogliomas, one oligoastrocytoma as diffuse astrocytoma, 4 diffuse astrocytomas as oligodendrogliomas, and 8 anaplastic oligoastrocytomas and 6 anaplastic astrocytomas as anaplastic oligodendrogliomas. A complete summary of demographic, clinical, and histomolecular data for all patients and each LGG type considered separately is shown in [Supplementary Table S1](#) and [Table 1](#).

### [<sup>11</sup>C]MET PET Qualitative and Semi-quantitative Analysis

The interobserver agreement between the first two readers was strong ( $\kappa$ : 0.826). In particular, discordance in visual image interpretation was present 11/153 cases.

Overall, qualitative analysis of [<sup>11</sup>C]MET PET scans revealed 111 (73%) positive and 42 (27%) negative studies. On negative [<sup>11</sup>C]MET PET exams, 32 (21%) lesions appeared isometabolic and 10 (6%) hypometabolic. [Supplementary Figure S1](#) shows three examples of hypermetabolic, isometabolic, and hypometabolic lesions.

[<sup>11</sup>C]MET uptake was more frequent in grade 3 compared to grade 2 LGGs (83% vs. 64% of cases, respectively, *p* = .009). Correlations between clinicopathological characteristics and PET qualitative analysis results are summarized in [Supplementary Table S2](#).

When considering WHO LGG types, [<sup>11</sup>C]MET uptake was more prevalent in oligodendrogliomas than *IDH*-mutant astrocytomas (87% vs. 50% of cases, respectively). Isometabolic lesions were more commonly grade 2 *IDH*-mutant astrocytomas than grade 3 *IDH*-mutant astrocytomas and grade 2 and 3 oligodendrogliomas (53% vs 18%, 18%, and 0% of cases, respectively). Hypometabolic gliomas mainly were grade 2 and 3 *IDH*-mutant astrocytomas, while were more rarely grade 2 and 3 oligodendrogliomas (9% and 17% vs. 2% and 3% of cases, respectively). A graphical summary of findings at qualitative [<sup>11</sup>C]MET PET evaluation concerning LGG type is shown in [Figure 1](#).

Semi-quantitative [<sup>11</sup>C]MET PET image analysis was performed in 151/153 patients. In the remaining two cases, semi-quantitative analysis was not possible due to technical problems.

The median values of  $TBR_{max}$  and  $TBR_{mean}$  in lesions visually classified according to the pattern of [<sup>11</sup>C]MET uptake as hypermetabolic, isometabolic, and hypometabolic differed significantly (2.67, 1.25, and 0.90 for  $TBR_{max}$ , respectively, *p* = .0001; 1.62, 0.95, and 0.62 for  $TBR_{mean}$ , respectively, *p* = .0001). According to PET qualitative evaluation, a summary of median  $TBR_{max}$  and  $TBR_{mean}$  values is provided in [Supplementary Table S3](#).

$TBR_{max}$  and  $TBR_{mean}$  values were significantly higher in WHO grade 3 LGGs compared to grade 2 lesions ([Supplementary Figure S2](#)).

We observed significant differences in median  $TBR_{max}$  and  $TBR_{mean}$  values between WHO LGG types ([Figure 2](#)). The median  $TBR_{max}$  was highest in grade 3 oligodendrogliomas and lowest in grade 2 *IDH*-mutant astrocytomas (= 3.20 and = 1.37, respectively). A complete summary of the semi-quantitative analysis concerning the WHO type is provided in [Supplementary Table S4](#).

Grade 3 LGGs had a significantly higher MTV concerning grade 2 tumors ([Supplementary Figure S3](#)).

Median MTV was significantly different in the two types, being higher in oligodendroglial neoplasms than in *IDH*-mutant astrocytomas (21.14 cm<sup>3</sup> vs. 10.03 cm<sup>3</sup>, respectively, *p* = .0197) ([Supplementary Figure S4](#) and [Supplementary Table S5](#)).

Out of 111 positive [<sup>11</sup>C]MET PET examinations, there was a spatial overlap between the MET PET-based and T2-FLAIR-based tumor volume in 83 (75%) cases. In the remaining 28 (25%) cases, PET-positive areas were present outside foci of altered FLAIR signal intensity. The presence of regions with increased [<sup>11</sup>C]MET uptake outside FLAIR alterations was positively associated with tumor grade and was more common for grade 3 than grade 2 lesions (36% vs 15% cases, respectively, *p* = .009). Two examples of [<sup>11</sup>C]MET PET and MRI discordance are presented in [Figure 3](#).

**Table 1** Summary of Demographic, Clinical, and Histomolecular Characteristics for All Patients and for LGG Types Considered Separately

Variable	All Types (n = 153)		<i>IDH</i> -Mutant, 1p/19q-Codeleted (n = 93)		<i>IDH</i> -Mutant, 1p/19q-Non Codeleted (n = 60)		P value
	N (%)	Median (IQR)	N (%)	Median (IQR)	N (%)	Median (IQR)	
Age at surgery		40 (31–49)		41 (34–50)		36 (28–46)	<b>.0149</b>
ECOG PS at surgery							.068
0	148 (97%)		88 (95%)		60 (100%)		
≥1	5 (3%)		5 (5%)		0		
Extent of resection (EOR)							.127
Complete	110 (72%)		71 (76%)		39 (65%)		
Incomplete	43 (28%)		22 (24%)		21 (35%)		
Adjuvant treatment							<b>&lt;.001</b>
None	66 (43%)		45 (51%)		21 (41%)		
RT-CT	21 (14%)		10 (11%)		11 (22%)		
CT	27 (17%)		25 (29%)		2 (4%)		
RT	25 (16%)		8 (9%)		17 (33%)		
NA	14		5		9		
MRI contrast enhancement							.064
Yes	32 (21%)		24 (26%)		8 (13%)		
No	121 (79%)		69 (74%)		52 (87%)		
2021 WHO grade							.479
2	87 (57%)		55 (59%)		32 (53%)		
3	66 (43%)		38 (41%)		28 (47%)		
Ki-67 (n = 151)		4% (3–8%)		4% (3–8%)		4% (3–6%)	.2475
<i>MGMT</i> promoter methylation (n = 138)							.237
Methylated	131 (95%)		85 (97%)		46 (92%)		
Nonmethylated	7 (5%)		3 (3%)		4 (8%)		
NA	15		5		10		
<i>TP53</i> mutation (n = 72)							<b>&lt;.001</b>
Yes	33 (46%)		3 (7.5%)		30 (94%)		
No	39 (54%)		37 (92.5%)		2 (6%)		
NA	81		53		28		
<i>ATRX</i> mutation (n = 61)							<b>&lt;.001</b>
Yes	37 (61%)		7 (23%)		30 (100%)		
No	24 (39%)		24 (77%)		0		
NA	92		62		30		

NA, not available.

Among the [<sup>11</sup>C]MET PET-positive lesions, 32/111 (29%) demonstrated MRI contrast uptake. In all cases, contrast-enhancing tumor volumes were inside MET PET-based tumor volumes.

### Assessment of Prognosis by [<sup>11</sup>C]MET PET and Clinicopathological Parameters

As of May 2021, the median follow-up time after surgery was 34.5 months (IQR 17.6–58.9 months). Two patients died due to postoperative complications, and 58 patients had

an imaging diagnosis of tumor recurrence or progression based on the RANO criteria. Among these, a histology-proven anaplastic transformation occurred in 11 cases.

Overall, the median PFS was 46.3 (IQR 25.7–105.8) months (Supplementary Figure S6). In patients with *IDH*-mutant, 1p/19q-codeleted oligodendrogliomas the median PFS was 53.5 (IQR 25.9–105.8) months, while in *IDH*-mutant astrocytomas the median PFS was 38.4 (IQR 24.2–60.4) months. PFS curves for the two LGG types did not differ significantly ( $p = .220$ ) (Supplementary Figure S7).

When considering all LGG patients, extent of resection and  $TBR_{max}$  were significantly associated with PFS on univariate

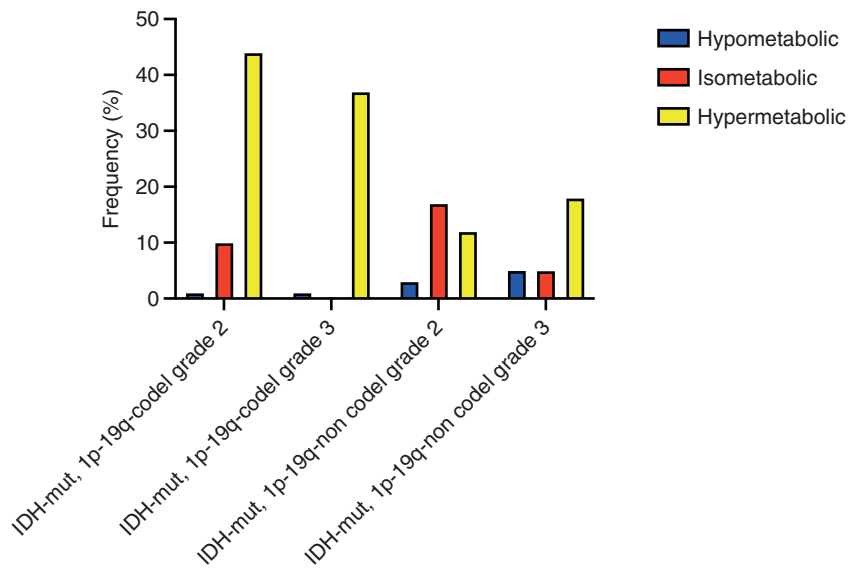


**Figure 1** [<sup>11</sup>C]MET PET qualitative analysis results by WHO LGG type.

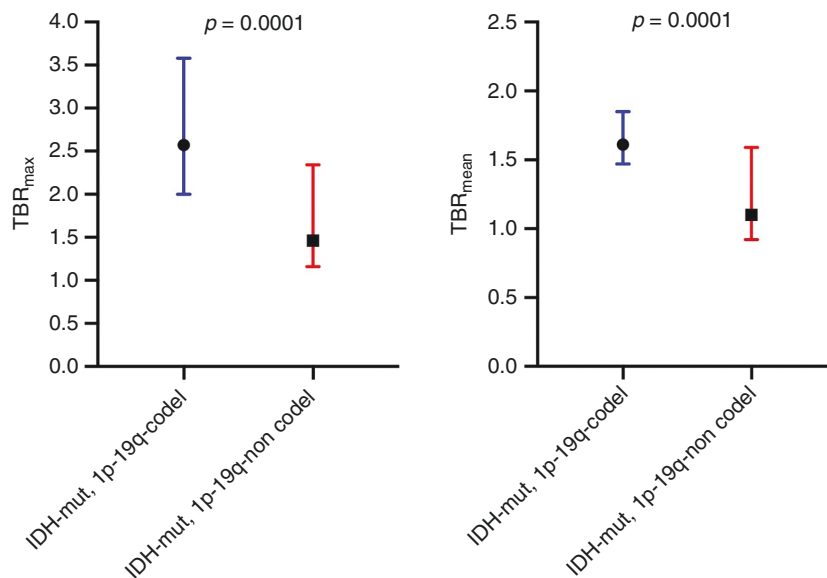


**Figure 2** [<sup>11</sup>C]MET PET semi-quantitative analysis results by WHO LGG type. Median TBR<sub>max</sub> (A), and TBR<sub>mean</sub> (B) values with interquartile ranges are shown for each type of LGG separately.

analysis and confirmed to be independent predictors of PFS on multivariate analysis (Supplementary Table S6). PFS curves for patients stratified according to extent of surgical resection and TBR<sub>max</sub> are shown in Supplementary Figure S8.

In *IDH*-mutant, 1p/19q-codeleted patients, extent of resection and postoperative treatment were significantly associated with PFS on univariate analysis; extent of

resection confirmed its independent prognostic value on multivariate analysis (Table 2).

In *IDH*-mutant astrocytomas, the extent of resection, TBR<sub>max</sub>, and TBR<sub>mean</sub> were significant predictors of PFS on univariate analysis. The extent of resection and TBR<sub>max</sub> confirmed their independent prognostic value on multivariate analysis (Table 3). PFS curves for *IDH*-mutant astrocytomas

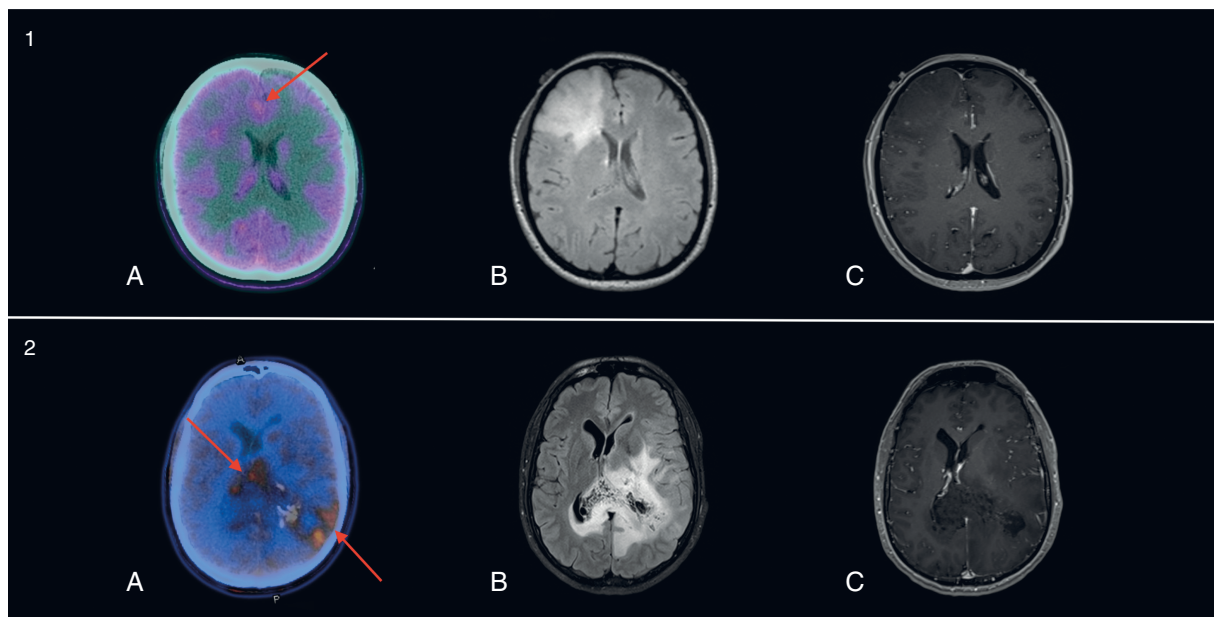


**Figure 3** Examples of lesions demonstrating increased [<sup>11</sup>C]MET uptake (red arrows) outside FLAIR alterations in (1) a 54-year-old patient with a right fronto-temporo-insular WHO grade 3 *IDH*-mutant astrocytoma; and (2) a 40-year-old patient with a bilateral thalamic and temporo-parietal WHO grade 3 oligodendroglioma. For each patient, (a) axial [<sup>11</sup>C]MET PET/CT, (b) axial T2-weighted FLAIR MRI images, and (c) axial postcontrast T1-weighted MRI images are shown.

stratified according to the extent of surgical resection and  $TBR_{max}$  are shown in [Figure 4](#).

## Discussion

The current study proved the added value of [<sup>11</sup>C]MET PET in the preoperative evaluation of a large cohort of newly diagnosed grade 2 and 3 glial neoplasms.

Regarding histopathological characteristics, we found that both visual analysis and semi-quantitative [<sup>11</sup>C]MET PET-derived parameters were significantly associated to tumor grade and LGG type. Indeed, [<sup>11</sup>C]MET uptake was more prevalent in grade 3 than grade 2 gliomas, and grade 3 lesions had higher  $TBR_{max}$  and  $TBR_{mean}$  values compared to grade 2 ones. Similar findings have been reported in previous studies.<sup>21–24</sup>

When looking at LGG types, the great majority (87%) of oligodendroglial tumors included in our cohort showed [<sup>11</sup>C]MET uptake and they exhibited the highest MTV and TBR values. Accordingly, the presence of a [<sup>11</sup>C]MET PET-negative lesion should support an alternative diagnosis. Conversely, *IDH*-mutant astrocytomas presented the lowest MTV and TBR values and were PET-negative in half of the patients. *IDH*-mutant astrocytomas represented 71% of all PET-negative lesions, in particular 80% and 69% of all hypometabolic and isometabolic tumors, respectively. Consequently, cold and isometabolic lesions at [<sup>11</sup>C]MET PET should raise the suspicion of these specific LGG entities. Our findings were in line with two previous reports by Kebir et al.<sup>25</sup> and Takei et al.,<sup>26</sup> who have described

a higher [<sup>11</sup>C]MET uptake in *IDH*-mutant, 1p/19q-codeleted LGGs compared to *IDH*-mutant, 1p/19q-non codeleted tumors. However, the small sample size in both these studies did not allow to find significant differences among LGG types with respect to radiopharmaceutical uptake.

Literature data suggested that higher cell and microvessels density are responsible for a different pattern of [<sup>11</sup>C]MET uptake in oligodendrogliomas and *IDH*-mutant astrocytomas.<sup>27–29</sup> More recently, Roodakker et al.<sup>30</sup> evaluated the intratumoral [<sup>11</sup>C]MET uptake according to tumor perfusion and histological protein expression and proved that different patterns of [<sup>11</sup>C]MET uptake featuring oligodendrogliomas and *IDH*-mutant astrocytomas were related to both tumor cell and microvessels density.

Secondly, we assessed the overlap between tumor volume measured on [<sup>11</sup>C]MET PET and on T2-FLAIR MRI, which is currently the preferred imaging method to delineate tumor margins before surgery in LGGs. PET-positive areas were present outside foci of altered FLAIR signal intensity in 25% of cases, supporting the independent and complementary role of these two techniques, already proved in gliomas of all grades by Pirotte et al.<sup>8</sup> The addition of PET to MRI data in the preoperative planning may help to extend the resection and target it to more aggressive areas, ultimately improving overall surgical outcomes. Moreover, Tanaka et al.<sup>10</sup> have reported that using a multimodal navigation system with integrated [<sup>11</sup>C]MET PET images to guide tumor resection improved survival in grades 2–4 gliomas patients concerning conventional navigation.

Coming to prognosis assessment, we aimed to determine whether [<sup>11</sup>C]MET PET is an independent prognostic factor in grade 2 and 3 glial neoplasms. Given the

**Table 2** Univariate and Multivariable Cox Regression Analysis of PFS for Oligodendrogliomas

Variable	Univariate Analysis			Multivariate Analysis		
	HR	95% CI	P value	HR	95% CI	P value
Sex (female vs. male)	0.844	0.401–1.776	.655			
Age	0.988	0.960–1.018	.435			
ECOG PS ( $\geq 1$ vs. 0)	NA					
Grade (grade 2 vs. grade 3)*	0.521	0.262–1.036	.063			
% Ki-67	1.027	0.991–1.063	.141			
MGMT prom methylation (yes vs. no)	NA					
EOR (complete vs. incomplete)*	0.351	0.169–0.727	<b>.005</b>	0.322	0.145–0.713	<b>.005</b>
Postoperative treatments (yes vs. no)*	2.100	1.042–4.233	<b>.038</b>			
Contrast enhancement (yes vs. no)	0.968	0.449–2.087	.934			
PET qualitative (PET+ vs. PET-)	1.476	0.518–4.210	.466			
TBR <sub>max</sub>	1.037	0.822–1.309	.756			
TBR <sub>mean</sub>	1.028	0.484–2.181	.943			

**Abbreviations:** CI, confidence interval; HR, hazard ratio; NA, not applicable as a stratification factor. Variables selected for the multivariate analysis are reported in bold.

\*Variables selected for the multivariate analysis.

**Table 3** Univariate and Multivariable Cox Regression Analysis of PFS for IDH-Mutant Astrocytomas

Variable	Univariate Analysis			Multivariate Analysis		
	HR	95% CI	P value	HR	95% CI	P value
Sex (female vs. male)	1.457	0.651–3.261	.360			
Age	1.028	0.999–1.059	.058			
ECOG PS ( $\geq 1$ vs. 0)	NA					
Grade (grade 2 vs. grade 3)*	1.439	0.627–3.306	.391			
% Ki-67	1.010	0.941–1.084	.790			
MGMT prom methylation (yes vs. no)	NA					
EOR (complete vs. incomplete)*	0.341	0.148–0.790	<b>.012</b>	0.292	0.101–0.848	<b>.023</b>
Postoperative treatments (yes vs. no)*	0.812	0.356–1.855	.622			
Contrast enhancement (yes vs. no)	0.396	0.0527–2.982	.369			
PET qualitative (PET+ vs. PET-)	2.062	0.896–4.742	.089			
TBR <sub>max</sub> *	1.827	1.395–2.394	<b>&lt;.001</b>	3.849	1.663–11.321	<b>.003</b>
TBR <sub>mean</sub> *	4.219	1.754–10.149	<b>.001</b>			

**Abbreviations:** CI, confidence interval; HR, hazard ratio; NA, not applicable as a stratification factor. Variables selected for the multivariate analysis are reported in bold.

\*Variables selected for the multivariate analysis.

tremendous heterogeneity across LGG subtypes in terms of biological behavior and prognosis, we carried out our analysis first in all patients, and then in patients stratified according to the LGG type.

Considering the whole LGG population, complete resection and lower TBR<sub>max</sub> values emerged as significant predictors of longer PFS on multivariate analysis, in agreement with most recent literature data.<sup>31–34</sup> Similarly, Poetsch et al.<sup>35</sup> have reported that TBR<sub>max</sub> on [<sup>11</sup>C]MET PET was an independent predictor of OS in a cohort of treatment-naïve grade 2–4 gliomas. More recently, a [<sup>11</sup>C]

MET PET-based radiomic analysis performed by Manabe et al.<sup>36</sup> on a small cohort of grade 2–4 gliomas has shown that two textural features (i.e. LGRE and correlation) derived from preoperative PET images were independent predictors of OS on multivariate analysis, while TBR<sub>max</sub> did not result to be independently associated to OS.

By restricting the evaluation to IDH-mutant, 1p/19q-codeleted patients, extent of resection was the only independent prognostic factor for PFS on multivariate analysis, in line with previous reports.<sup>32,37,38</sup> On the other hand, visual [<sup>11</sup>C]MET uptake and



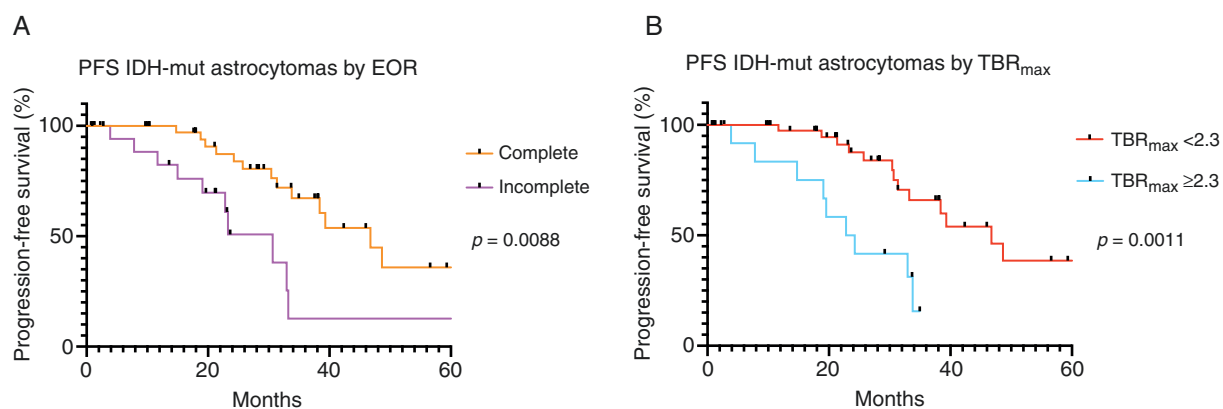


**Figure 4** Kaplan-Meier curves for PFS for *IDH*-mutant astrocytomas stratified according to extent of surgical resection (A) and  $TBR_{max}$  (B). \*variables selected for the multivariate analysis. CI, confidence interval; HR, hazard ratio; NA, not applicable as a stratification factor.

semi-quantitative parameters were not significantly associated with PFS, suggesting that their prognostic role in oligodendrogliomas is limited.

Looking at the *IDH*-mutant, 1p/19q-non codeleted type, complete tumor resection, and increasing  $TBR_{max}$  values demonstrated to be independent predictors of shorter PFS on multivariate Cox regression analysis. Similarly, several recent studies<sup>32,39–41</sup> have shown that extensive surgery was independently associated with better survival outcomes in *IDH*-mutant astrocytomas. To the best of our knowledge, instead, the role of  $TBR_{max}$  on [<sup>11</sup>C]MET PET in this specific LGG type as an independent predictor of survival has never been reported before.

The present work demonstrates that preoperative [<sup>11</sup>C]MET PET is a valuable diagnostic and prognostic tool in grade 2 and 3 glial neoplasms. Unlike most former studies, which had included patients with glial neoplasms of all grades, we centered our analysis only on lower-grade gliomas. Moreover, this is the first comprehensive investigation on the prognostic value of amino acid PET in LGG stratified according to 2021 WHO diffuse glioma type and other known prognostic factors. Following the 2016 and 2021 CNS WHO recommendations, such stratification based on *IDH1/2* genes mutation and 1p/19q codeletion has become fundamental to evaluate the impact of prognostic factors on survival outcomes without introducing sample bias. *IDH*-mutant, 1p/19q-codeleted, and *IDH*-mutant, 1p/19q-non codeleted LGGs are indeed distinct entities with dissimilar phenotypic and genotypic characteristics and different natural history and response to treatment.

Current guidelines for imaging of gliomas recommends the use of PET with radiolabeled amino acids.<sup>14</sup> Our data further support this recommendation, with several practical applications both in the pre- and postsurgical setting. In particular, we expanded knowledge about the usefulness of [<sup>11</sup>C]MET PET for (a) estimation of lower-grade glioma type; (b) delineation of tumor extent for surgery; and (c) prognostication of lower-grade gliomas.

First, we proved the usefulness of [<sup>11</sup>C]MET PET for the prospective assessment of LGG type and grade. It holds the potential of providing considerable improvements in the preoperative estimation of tumor biological characteristics before the availability of a histomolecular diagnosis. Several studies<sup>32,37,40</sup> have shown how the extent of surgical resection impacted outcome based on LGG type. In particular, the *IDH*-mutant, 1p/19q-non codeleted subgroup maximally benefitted from increased EOR. In light of this, [<sup>11</sup>C]MET PET may guide treatment decision-making in these patients, supporting a more aggressive surgical approach in case of lesions highly suspicious for *IDH*-mutant astrocytomas.

Additionally, we demonstrated the complementary role of MRI and [<sup>11</sup>C]MET PET in delineating tumor margins before LGG surgery. Therefore, the use of a multimodal navigation system integrating the information from [<sup>11</sup>C]MET PET and MRI may help to better plan surgery, increase the amount of tumor removed, and target—whenever possible—the resection to more active tumor portions.

Finally, for the first time, our findings proved the independent prognostic role of [<sup>11</sup>C]MET PET in LGG patients with *IDH*-mutant astrocytomas. Previous studies<sup>35,36,42–48</sup> have evidenced the association between preoperative amino acid (i.e. [<sup>11</sup>C]MET, [<sup>18</sup>F]FET, and [<sup>18</sup>F]DOPA) PET and clinical outcome both in low- and high-grade gliomas. However, none of these has stratified patients according to molecular subtype and has performed adjustment for known prognostic factors in glial neoplasms.

Our results supported the utilization of [<sup>11</sup>C]MET PET to personalize treatment decisions in *IDH*-mutant, 1p/19q-noncodeleted LGGs. Accordingly, we propose to use high  $TBR_{max}$  values at preoperative [<sup>11</sup>C]MET PET to select high-risk patients for closer monitoring and more aggressive treatment strategies after surgery.

Despite the relatively large sample size and the further stratification of patients in molecularly defined subgroups, our study needs to acknowledge some limitations. First, some histomolecular data (Ki-67 index, *MGMT* promoter methylation, *ATRX*, and *TP53* status) were not available for

all patients due to the retrospective design. A further limitation is represented by the binary stratification of the extent of surgical resection (complete and incomplete) instead of a volumetric approach, which would have been more accurate. Moreover, the small number of hypometabolic lesions in our LGG cohort did not allow us to investigate the prognostic value of “cold” areas, which have been recently correlated with unfavorable outcomes.<sup>49,50</sup> Additionally, correlation of clinicopathological and imaging data with overall survival was not analyzed; indeed, follow-up was too short considering the relatively long median survival of patients with LGGs. Moreover, as it can be difficult to differentiate LGGs from other brain tumors in the preoperative setting, the validity of [<sup>11</sup>C]MET PET for noninvasive subtype classification should be considered with caution. Lastly, [<sup>11</sup>C]MET PET is currently restricted to few neuro-oncology centers because the short half-life of <sup>11</sup>C (20 minutes) necessitates an onsite cyclotron. In Europe, [<sup>11</sup>C]MET has indeed been replaced by [<sup>18</sup>F]FET and [<sup>18</sup>F]FDOPA.<sup>51</sup> However, since MET, FET, and FDOPA are transported by the same amino acid transport system L, concordance among these radiolabeled amino acids in diagnostic findings is expected.<sup>14</sup>

In conclusion, the present study highlights the added value of preoperative [<sup>11</sup>C]MET PET in estimating molecular features in suspected LGGs, assessing tumor extent, and providing independent prognostic information in patients with histologically confirmed lower-grade gliomas. Our results support the routine implementation of amino acid PET with [<sup>11</sup>C]methionine to personalize treatment decisions and optimize patient management in newly diagnosed grade 2 and 3 glial neoplasms.

## Supplementary material

Supplemental material is available at *Neuro-Oncology* online.

## Keywords

brain tumors | lower-grade gliomas | [<sup>11</sup>C]methionine PET | prognosis | surgery

## Acknowledgments

The authors are thankful to Prof. Lorenzo Bello, Dr Maurizio Fornari, Dr Marco Grimaldi, Dr Giovanni Battista Lasio for their clinical support.

**Conflict of interest statement.** Arturo Chiti reports: speaker's honoraria: Advanced Accelerator Applications, General Electric Healthcare, AmGen Europe; Advisory Boards: Blue Earth Diagnostics, Advanced Accelerator Applications. The other authors do not report any conflict of interest.

**Authorship statement.** F.P., G.N., P.N., M.S., and A.C. ideated the project; P.N., F.P., B.B., L.A., L.S.P., and F.G. extracted and analyzed the data, N.G. and D.F. provided the statistical analyses; G.N., F.P., M.S., and A.C. prepared the draft, all authors read and approved the text.

## References

- Ostrom QT, Patil N, Cioffi G, et al. CBTRUS statistical report: Primary brain and other central nervous system tumors diagnosed in the United States in 2013-2017. *Neuro Oncol* 2020;22(12 Suppl 2):iv1–iv96.
- Louis DN, Ohgaki H, Wiestler OD, et al. The 2007 WHO classification of tumors of the central nervous system. *Acta Neuropathol.* 2007;114(2):97–109.
- Louis DN, Perry A, Reifenberger G, et al. The 2016 World Health Organization Classification of Tumors of the Central Nervous System: a summary. *Acta Neuropathol.* 2016;131(6):803–820.
- Louis DN, Perry A, Wesseling P, et al. The 2021 WHO Classification of Tumors of the Central Nervous System: a summary. *Neuro Oncol* 2021;23(8):1231–1251.
- Louis DN, Wesseling P, Aldape K, et al. cIMPACT-NOW update 6: new entity and diagnostic principle recommendations of the cIMPACT-Utrecht meeting on future CNS tumor classification and grading. *Brain Pathol.* 2020;30(4):844–856. doi:10.1111/bpa.12832.
- Cancer Genome ARN, Brat DJ, Verhaak RG, et al. Comprehensive, integrative genomic analysis of diffuse lower-grade gliomas The Cancer Genome Atlas Research Network. *N Engl J Med.* 2015;372(26):2481–98.
- Van Den Bent MJ, Weller M, Wen PY, et al. clinical perspective on the 2016 WHO brain tumor classification and routine molecular diagnostics. *Neuro Oncol* 2017;19(5):614–624.
- Pirotte B, Goldman S, Dewitte O, et al. Integrated positron emission tomography and magnetic resonance imaging-guided resection of brain tumors: a report of 103 consecutive procedures. *J Neurosurg.* 2006;104(2):238–53.
- Kracht LW, Miletic H, Busch S, et al. Delineation of brain tumor extent with [<sup>11</sup>C]L-methionine positron emission tomography: local comparison with stereotactic histopathology. *Clin Cancer Res.* 2004;10:7163–7170.
- Tanaka Y, Nariai T, Momose T, et al. Glioma surgery using a multimodal navigation system with integrated metabolic images. *J Neurosurg.* 2009;110(1):163–172.
- Kunz M, Thon N, Eigenbrod S, et al. Hot spots in dynamic 18F-FET-PET delineate malignant tumor parts within suspected WHO grade II gliomas. *Neuro Oncol* 2011;13(3):307–316.
- Pafundi DH, Laack NN, Youland RS, et al. Biopsy validation of 18F-DOPA PET and biodistribution in gliomas for neurosurgical planning and radiotherapy target delineation: results of a prospective pilot study. *Neuro Oncol* 2013;15(8):1058–67.
- Albert NL, Weller M, Suchorska B, et al. Response Assessment in Neuro-Oncology working group and European Association for Neuro-Oncology recommendations for the clinical use of PET imaging in gliomas. *Neuro Oncol* 2016;18(9):1199–208.
- Law I, Albert NL, Arbizu J, et al. Joint EANM/EANO/RANO practice guidelines/SNMMI procedure standards for imaging of gliomas using PET with radiolabelled amino acids and [<sup>18</sup>F]FDG: version 1.0. *Eur J Nucl Med Mol Imaging.* 2019;46:540–557.

15. Näslund O, Smits A, Förander P, et al. Amino acid tracers in PET imaging of diffuse low-grade gliomas: a systematic review of preoperative applications. *Acta Neurochir (Wien)* 2018;160:1451–1460.
16. Unterrainer M, Vettermann F, Brendel M, et al. Towards standardization of <sup>18</sup>F-FET PET imaging: Do we need a consistent method of background activity assessment? *EJNMMI Res* 2017;7:1–8.
17. Nioche C, Orlhac F, Boughdad S, et al. Lifex: a freeware for radiomic feature calculation in multimodality imaging to accelerate advances in the characterization of tumor heterogeneity. *Cancer Res* 2018;78(16):4786–4789.
18. Wen PY, Macdonald DR, Reardon DA, et al. Updated response assessment criteria for high-grade gliomas: response assessment in neuro-oncology working group. *J Clin Oncol* 2010;28(11):1963–1972.
19. Van den Bent MJ, Wefel JS, Schiff D, et al. Response assessment in neuro-oncology (a report of the RANO group): assessment of outcome in trials of diffuse low-grade gliomas. *Lancet Oncol* 2011;12(6):583–593.
20. McHugh ML. Lessons in biostatistics interrater reliability: the kappa statistic. *Biochem Medica* 2012;22(3):276–282.
21. Kim D, Chun JH, Kim SH, et al. Re-evaluation of the diagnostic performance of <sup>11</sup>C-methionine PET/CT according to the 2016 WHO classification of cerebral gliomas. *Eur J Nucl Med Mol Imaging* 2019;46:1678–1684.
22. Nariai T, Tanaka Y, Wakimoto H, et al. Usefulness of L-[methyl-<sup>11</sup>C]methionine-positron emission tomography as a biological monitoring tool in the treatment of glioma. *J Neurosurg* 2005;103(3):498–507.
23. Ogawa T, Kawai N, Miyake K, et al. Diagnostic value of PET/CT with <sup>11</sup>C-methionine (MET) and <sup>18</sup>F-fluorothymidine (FLT) in newly diagnosed glioma based on the 2016 WHO classification. *EJNMMI Res* 2020;10(1):1–10.
24. Tarun S, Tanjore KN, Martin PJ, Chandrashekar B, Mantil JC. <sup>11</sup>C-methionine PET for grading and prognostication in gliomas: a comparison study with <sup>18</sup>F-FDG PET and contrast enhancement on MRI. *J Nucl Med* 2012;53(11):1709–1715.
25. Kebir S, Weber M, Lazaridis L, et al. Hybrid <sup>11</sup>C-MET PET/MRI combined with “machine learning” in glioma diagnosis according to the revised glioma WHO Classification 2016. *Clin Nucl Med* 2019;44(3):214–220.
26. Takei H, Shinoda J, Ikuta S, et al. Usefulness of positron emission tomography for differentiating gliomas according to the 2016 World Health Organization classification of tumors of the central nervous system. *J Neurosurg* 2020;16:1–10.
27. Langen K-J, Rapp M, Sabel M, Galldiks N. Positron-Emission-Tomography in Diffuse Low-Grade Gliomas. In: Duffau H, ed. *Diffuse Low-Grade Gliomas in Adults*. Cham: Springer; 2017:263–286.
28. Chan A, Leung S, Wong M, et al. Expression of vascular endothelial growth factor and its receptors in the anaplastic progression of astrocytoma, oligodendroglioma, and ependymoma. *Am J Surg Pathol* 1998;22(7):816–826.
29. Kracht LW, Friese M, Herholz K, et al. Methyl-[<sup>11</sup>C]-L-methionine uptake as measured by positron emission tomography correlates to microvessel density in patients with glioma. *Eur J Nucl Med Mol Imaging* 2003;30(6):868–873.
30. Roodakker KR, Alhuseinalkhudhur A, Al-Jaff M, et al. Region-by-region analysis of PET, MRI, and histology in en bloc-resected oligodendrogliomas reveals intra-tumoral heterogeneity. *Eur J Nucl Med Mol Imaging* 2019;46(3):569–579.
31. Hervey-Jumper SL, Berger MS. Evidence for improving outcome through extent of resection. *Neurosurg Clin N Am* 2019;30(1):85–93.
32. Patel SH, Bansal AG, Young EB, et al. Extent of surgical resection in lower-grade gliomas: differential impact based on molecular subtype. *Am J Neuroradiol* 2019;40(7):1149–1155.
33. Gittleman H, Sloan AE, Barnholtz-Sloan JS. An independently validated survival nomogram for lower-grade glioma. *Neuro Oncol* 2020;22(5):665–674.
34. Choi J, Kim SH, Ahn SS, et al. Extent of resection and molecular pathologic subtype are potent prognostic factors of adult WHO grade II glioma. *Sci Rep* 2020;10(1):2086.
35. Poetsch N, Woehrer A, Gesperger J, et al. Visual and semiquantitative <sup>11</sup>C-methionine PET: An independent prognostic factor for survival of newly diagnosed and treatment-naïve gliomas. *Neuro Oncol* 2018;20(3):411–419.
36. Manabe O, Yamaguchi S, Hirata K, et al. Preoperative texture analysis using <sup>11</sup>C-methionine positron emission tomography predicts survival after surgery for glioma. *Diagnostics* 2021;11(189):1–9.
37. Wijnenga MMJ, French PJ, Dubbink HJ, et al. The impact of surgery in molecularly defined low-grade glioma: an integrated clinical, radiological, and molecular analysis. *Neuro Oncol* 2018;20(1):103–112.
38. Garton ALA, Kinslow CJ, Rae AI, et al. Extent of resection, molecular signature, and survival in 1p19q-codeleted gliomas. *J Neurosurg* 2020;134(May):1–11.
39. Wijnenga MMJ, French PJ, Dubbink HJ, et al. The impact of surgery in molecularly defined low-grade glioma: an integrated clinical, radiological, and molecular analysis. *Neuro Oncol* 2018;20(1):103–112.
40. Kawaguchi T, Sonoda Y, Shibahara I, et al. Impact of gross total resection in patients with WHO grade III glioma harboring the IDH 1/2 mutation without the 1p/19q co-deletion. *J Neurooncol* 2016;129(3):505–514.
41. Kavouridis VK, Boaro A, Dorr J, et al. Contemporary assessment of extent of resection in molecularly defined categories of diffuse low-grade glioma: a volumetric analysis. *J Neurosurg* 2020;133(5):1291–1301.
42. Smits A, Westerberg E, Ribom D. Adding <sup>11</sup>C-methionine PET to the EORTC prognostic factors in grade 2 gliomas. *Eur J Nucl Med Mol Imaging* 2008;35(1):65–71.
43. Villani V, Carapella CM, Chiaravalloti A, et al. The role of PET [<sup>18</sup>F]FDOPA in evaluating low-grade glioma. *Anticancer Res* 2015;35(9):5117–5122.
44. Oughourlian TC, Yao J, Schlossman J, et al. Rate of change in maximum <sup>18</sup>F-FDOPA PET uptake and non-enhancing tumor volume predict malignant transformation and overall survival in low-grade gliomas. *J Neurooncol* 2020;147(1):135–145.
45. Chiaravalloti A, Esposito V, Ursini F, et al. Overall survival and progression-free survival in patients with primary brain tumors after treatment: is the outcome of [<sup>18</sup>F] FDOPA PET a prognostic factor in these patients? *Ann Nucl Med* 2019;33(7):471–480.
46. Thon N, Kunz M, Lemke L, et al. Dynamic <sup>18</sup>F-FET PET in suspected WHO grade II gliomas defines distinct biological subgroups with different clinical courses. *Int J Cancer* 2015;136(9):2132–2145.
47. Jansen NL, Suchorska B, Wenter V, et al. Dynamic <sup>18</sup>F-FET PET in newly diagnosed astrocytic low-grade glioma identifies high-risk patients. *J Nucl Med* 2014;55(2):198–203.
48. Lopci E, Riva M, Olivari L, et al. Prognostic value of molecular and imaging biomarkers in patients with supratentorial glioma. *Eur J Nucl Med Mol Imaging* 2017;44(7):1155–1164.
49. Galldiks N, Unterrainer M, Judov N, et al. Photopenic defects on O-(2-[<sup>18</sup>F]-fluoroethyl)-L-tyrosine PET: Clinical relevance in glioma patients. *Neuro Oncol* 2019;21(10):1331–1338.
50. Galldiks N, Verger A, Zaragori T, et al. Comment on “Hypometabolic gliomas on FET-PET-is there an inverted U-curve for survival?”. *Neuro Oncol* 2019;21(12):1612–1613.
51. Langen KJ, Galldiks N, Hattingen E, Shah NJ. Advances in neuro-oncology imaging. *Nat Rev Neurol* 2017;13(5):279–289.